

Mechanism of oxide thickness and temperature dependent current conduction in n^+ -polySi/SiO₂/p-Si structures — a new analysis

Piyas Samanta[†]

Department of Physics, Vidyasagar College for Women, 39 Sankar Ghosh Lane, Kolkata 700006, India

Abstract: The conduction mechanism of gate leakage current through thermally grown silicon dioxide (SiO₂) films on (100) p-type silicon has been investigated in detail under negative bias on the degenerately doped n-type polysilicon (n^+ -polySi) gate. The analysis utilizes the measured gate current density J_G at high oxide fields E_{ox} in 5.4 to 12 nm thick SiO₂ films between 25 and 300 °C. The leakage current measured up to 300 °C was due to Fowler–Nordheim (FN) tunneling of electrons from the accumulated n^+ -polySi gate in conjunction with Poole Frenkel (PF) emission of trapped-electrons from the electron traps located at energy levels ranging from 0.6 to 1.12 eV (depending on the oxide thickness) below the SiO₂ conduction band (CB). It was observed that PF emission current I_{PF} dominates FN electron tunneling current I_{FN} at oxide electric fields E_{ox} between 6 and 10 MV/cm and throughout the temperature range studied here. Understanding of the mechanism of leakage current conduction through SiO₂ films plays a crucial role in simulation of time-dependent dielectric breakdown (TDDDB) of metaloxide–semiconductor (MOS) devices and to precisely predict the normal operating field or applied gate voltage for lifetime projection of the MOS integrated circuits.

Key words: FN tunneling; PF emission; image force lowering; trap depth

DOI: 10.1088/1674-4926/38/10/104001

PACS: 72.20.Jv; 73.40.Gk; 73.40.Qv

1. Introduction

The current conduction through SiO₂ gate dielectric is crucial for its successful application in metal–oxide–semiconductor (MOS) devices. Because of the large electron energy barrier Φ_B at the Si/SiO₂ interface and low trap density in the oxide forbidden gap, the dominant current conduction mechanism in silicon based MOS devices was believed to be the electrode-limited conduction^[1] via Fowler–Nordheim (FN)^[2–5] or direct tunneling (DT)^[6] depending on the oxide thickness t_{ox} and applied oxide voltage V_{ox} . The electronic current conduction through SiO₂ films thicker than 5 nm and at oxide electric fields E_{ox} above 6 MV/cm satisfying $V_{ox} > \Phi_B$ is widely accepted to be solely due to FN tunneling of electrons from the inversion or accumulation layer of silicon substrate or polysilicon gate through the triangular energy barrier at the cathode/oxide interface^[4, 6]. FN tunneling current is a major concern for the reliability of MOS structures as well as for the functionality of electrically erasable programmable read-only memory (EEPROM) devices at room temperature^[4] and also at elevated temperatures^[7]. Therefore, since early 1970s FN tunneling mechanism has been received much attention by several researchers^[2–10].

In earlier reports^[2–5], current conduction mechanism through SiO₂ dielectric in MOS structures at room temperature was established as the FN tunneling of electrons from the excellent linear fit of the measured $\ln(J_G E_{ox}^2)$ versus $1/E_{ox}$ data as demanded by the Lenzlinger–Snow (LS) equation^[2].

$$J_G = A_{FN} E_{ox}^2 \exp(-B_{FN}/E_{ox}), \quad (1)$$

where J_G is the current density, E_{ox} is the oxide electric field, B_{FN} and A_{FN} are FN constants given by^[4]

$$B_{FN} = \frac{4}{3} \sqrt{\frac{2q m_{ox} \Phi_B^3}{\hbar^2}}, \quad (2)$$

$$A_{FN} = \frac{q^2 m_{Si}}{16\pi^2 \hbar \Phi_B m_{ox}}, \quad (3)$$

where $m_{ox} = 0.42m_0$ and $m_{Si} = 0.916m_0$ are the effective masses of the electron in oxide^[2] and in silicon normal to the interface^[3], respectively, m_0 is the free electron mass, \hbar is the reduced Planck's constant, q is the magnitude of electron charge, and Φ_B is the effective electron barrier height^[7] at the cathode/oxide interface measured from the Fermi level E_F of the cathode. Φ_B is related to the conduction band offset^[11] Φ_c^c by $\Phi_B = \Phi_c^c - (E_F - E_c)$, where E_c is the conduction band edge in eV as shown in the inset in Fig. 1(a). Incorporating the temperature variations empirically in B_{FN} and A_{FN} , the above LS Eq. (1) has also been used by other researchers to explain the current conduction in MOS devices as FN tunneling at elevated temperatures^[7–10]. However, the validity of the LS Eq. (1) originally developed^[2] for electron emission from the metal electrode at 0 K becomes questionable^[11] while used in explaining tunnel injection of electrons from the semiconductor surface. To resolve the above debate, we therefore have developed a closed form expression for FN tunnel injection from the accumulation layer of the semiconductor surface at a wide range of temperatures. Moreover, the excellent numerical fit of the measured data with Eq. (1) cannot ensure

[†] Corresponding author. Email: piyas@vcfw.org

Received 23 November 2016, revised manuscript received 30 April 2017

©2017 Chinese Institute of Electronics

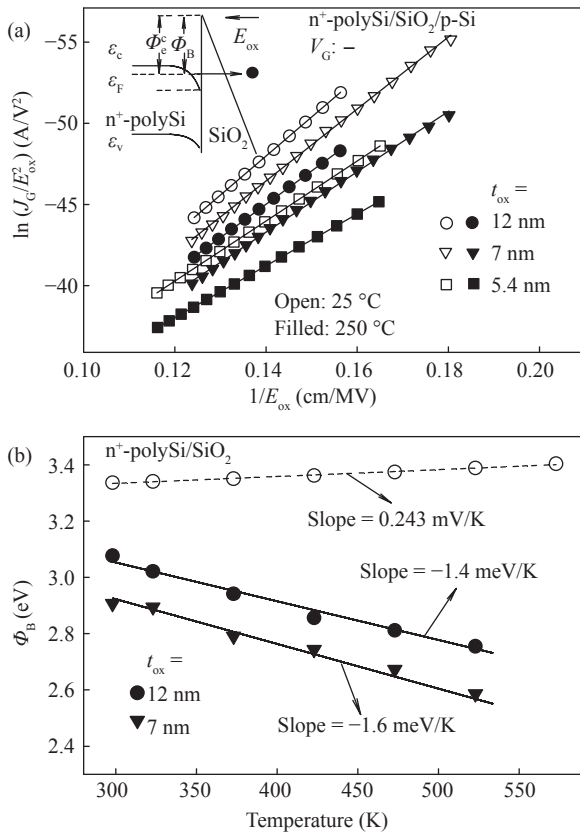


Fig. 1. (a) Fowler–Nordheim (FN) plot of the measured^[8] leakage current density J_G during electron injection from n^+ -polySi gate into thermally grown thin SiO_2 films in as-grown MOS capacitors on p-Si with oxide thickness and temperature as parameters. Curves are fits to LS Eq. (1) and symbols are from experiment^[8]. Inset shows the schematic band diagram of FN tunneling of electrons through the effective triangular barrier energy Φ_B (measured from the Fermi level in accumulated n^+ -polySi) at the interface. (b) Temperature variation of the effective electron barrier height Φ_B at the n^+ -polySi/ SiO_2 interface determined from the FN slope B_{FN} of the measured^[8] J_G versus E_{ox} data for different oxide thicknesses (filled symbols). Also shown are the theoretically estimated (open circles) results considering temperature dependent Fermi level incomplete ionization of the dopant atoms in n^+ -polySi using FD statistics.

the conduction mechanism solely due to FN tunneling of electrons as will be elaborated below.

Furthermore, understanding the current conduction mechanism is crucial in studying hot-electron induced anode hole injection (AHI) and related oxide degradation particularly in thin SiO_2 films down to 15 nm as originally proposed by Samanta and co-worker^[12, 13] for 4H-SiC devices. The present work is therefore a first time attempt to critically investigate the mechanism(s) of oxide thickness t_{ox} dependent current conduction through thin SiO_2 films in n^+ -polySi/ SiO_2 /p-Si diodes at high fields and temperatures with an aim to theoretically study the time-dependent dielectric breakdown (TDDB) in silicon based MOS devices.

2. Device details

The devices studied here were n^+ -polySi gate tunnel oxide MOS capacitors having 5.4-, 7-, 9- and 12-nm thick SiO_2

films thermally grown on (100) oriented p-Si. Acceptor dopant concentrations of the substrates were $1.2 \times 10^{15} \text{ cm}^{-3}$ for 5.4-, 7- and 12-nm thick and $6 \times 10^{17} \text{ cm}^{-3}$ for 9-nm thick SiO_2 films, respectively. Phosphorous donor concentration (N_D) in n^+ -polySi gate was 10^{20} cm^{-3} . Details of device process flow are found elsewhere^[8]. Current–voltage measurements were carried out by Hadjadj and co-workers^[8] keeping p-Si in accumulation condition (negative bias on n^+ -polySi gate) at a wide range of temperatures between 25 and 300 °C.

3. Analysis and discussions

3.1. Current conduction mechanism

The excellent fit of the measured^[8] J_G versus E_{ox} data with the conventional LS Eq. (1) irrespective of oxide thickness and temperature as shown in Fig. 1(a) apparently indicates FN tunneling of electrons to occur from the n^+ -polySi gate at a wide range of temperatures. However, FN tunneling current density J_G modeled by the LS Eq. (1) is essentially oxide thickness independent when considered at a given applied electric field E_{ox} . Therefore, FN tunneling is unlikely the primary conduction mechanism to explain the observed t_{ox} dependence of J_G at a given applied electric field E_{ox} and temperature in Fig. 1(a). The effective electron barrier height Φ_B at the injecting electrode/oxide interface is usually estimated from the slope B_{FN} of the experimental $\ln(J_G/E_{\text{ox}}^2)$ versus $1/E_{\text{ox}}$ linear FN plot and using Eq. (2). Both theoretical and experimental results of the temperature variations of Φ_B are shown in Fig. 1(b). Contrary to the results of Φ_B estimated using experimental J_G – E_{ox} data, our theoretical calculation clearly shows that Φ_B increases with increasing temperature due to the combined effects of increasing Φ_c^e and the Fermi level with increasing temperature for a given dopant concentration in the n^+ -polySi cathode. Moreover, there is no physical reason of the t_{ox} dependence of Φ_B as estimated at a given temperature [Fig. 1(b)]. t_{ox} independent theoretical values of Φ_B were calculated using temperature variation of the conduction band offset Φ_c^e schematically depicted in Fig. 2(a) and incomplete ionization^[14] of the dopant using Fermi-Dirac (FD) carrier statistics in n^+ -polySi.

Temperature dependence of Φ_c^e occurs due to unequal downshifts of the CBs of the n^+ -polySi and the SiO_2 caused due to spreading of the Urbach tail towards the midgap without any experimentally observed^[16] shift of the valence band (VB) top as schematically depicted in the inset (right) in Fig. 2(a). Taking both thermal narrowing^[14, 17] of intrinsic gaps and temperature dependent ionized dopant-induced bandgap narrowing^[18], the estimated bandgaps of n^+ -polySi and SiO_2 are listed in Table 1 along with the electron barrier height Φ_c^e (also called the CB offset) at the cathode (n^+ -polySi)/oxide interface. In order to estimate Φ_c^e , we have taken its measured^[15] value of 3.29 eV for nominal doping at room temperature. This value of CB offset for nominal doping is close to 3.25 eV reported in Ref. [14]. The small increase in Φ_c^e with increasing temperature (Table 1) is due to the smaller temperature-induced CB downshift in SiO_2 than that in n^+ -polySi, consistent with their measured^[14] thermal conductivities, which are correlated to the relative bond length change due to

Table 1. Temperature dependent bandgap E_g and electron barrier height at the cathode (n^+ -polySi) having $N_D = 10^{20} \text{ cm}^{-3}$.

Temperature ($^{\circ}\text{C}$)	E_g (n^+ -polySi)(eV)	E_g (SiO_2)(eV)	Φ_e^c (eV)
25	1.004	8.900	3.334
100	1.015	8.883	3.339
200	0.980	8.859	3.348
300	0.944	8.847	3.359

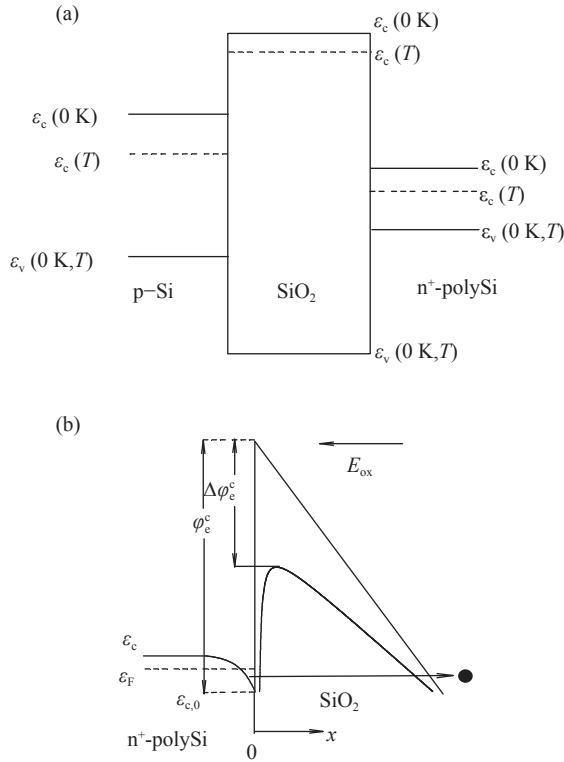


Fig. 2. Schematic band diagram illustrating (a) thermal narrowing of bandgaps of n^+ -polySi and SiO_2 due to downward shifts of the CBs towards midgap, while the valence bands are aligned^[15] and (b) FN tunneling of electrons below the CB edge of accumulated n^+ -polySi through the triangular energy barrier at the n^+ -polySi/ SiO_2 interface incorporating image force barrier lowering.

thermal expansion.

The above discussions critically examine the limitations of the widely used LS Eq. (1) in identifying the thickness and temperature dependent conduction mechanism through thin SiO_2 films used in MOS devices, even though a large class of J_G versus E_{ox} data can be empirically fitted with Eq. (1) yielding unphysical parameters. One should note that the above LS Eq. (1) originally derived^[2] for electron emission from the metal electrode at 0 K is no longer valid for field emission from a semiconductor at room temperature and above^[11] where a significant contribution in tunneling comes from the electrons residing below the CB edge due to band bending at the interface as schematically shown in Fig. 2(b). This physical idea necessitates redefining the electron barrier height by the CB offset Φ_e^c . Because of small band bending of the accumulation layer at the semiconductor (cathode)/oxide interface with an assumption of the classical 3D Fermi gas model, FN tunneling current density J_{FN} can be calculated by

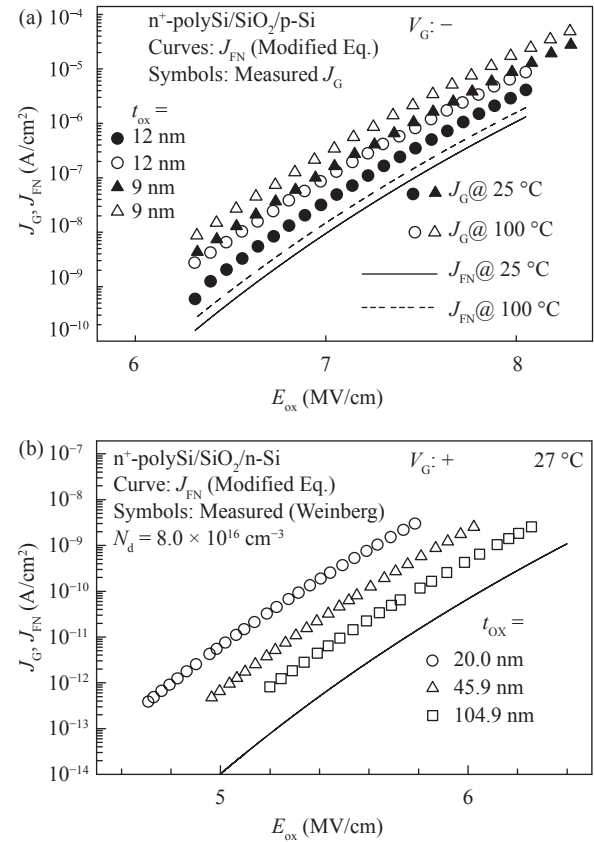


Fig. 3. Applied oxide field dependence of FN current density J_{FN} (curves) calculated using Eq. (5) and (a) measured^[8] (symbols) leakage current density J_G during electron injection from n^+ -polySi in as-grown MOS devices with oxide thickness and temperature as parameters. (b) Measured^[3] (symbols) leakage current density J_G during electron injection at room temperature from n -Si in as-grown MOS devices with oxide thickness as a parameter.

$$J_{FN} = \frac{qm_{Si}k_B T}{2\pi^2\hbar^3} \int_{\mathcal{E}_x=\mathcal{E}_{c,0}}^{\infty} d\mathcal{E}_x T_{WKB}(\mathcal{E}_x) \times \ln[1 + \exp(\mathcal{E}_F - \mathcal{E}_x)/k_B T], \quad (4)$$

where \mathcal{E}_F and $\mathcal{E}_{c,0}$ are the semiconductor Fermi level and the CB edge at the semiconductor (cathode)/oxide interface, respectively as shown in Fig. 2(b), k_B is the Boltzmann constant and T is the absolute temperature. Taking image force barrier lowering as schematically shown in Fig. 2(b) into account in calculating the tunneling transmission probability $T_{WKB}(\mathcal{E}_x)$ using Wenzel-Kramers-Brillouin (WKB) approximation, after involved algebraic manipulation Eq. (4) reduces to the following analytical form

$$J_{FN} = A' f(c) E_{ox}^2 \exp(-B'/E_{ox}), \quad (5)$$

$$c = t(y) \frac{2k_B T \sqrt{2m_{ox}\Phi_e^c/q}}{\hbar E_{ox}},$$

$$A' = A'_{FN}/t^2(y), \quad B' = B'_{FN}v(y),$$

$$f(c) = e^{-\eta c} [{}_2F_1(1, -c; 1 - c; -e^\eta) - c \ln(1 + e^\eta) - 1],$$

where B'_{FN} and A'_{FN} are obtained upon replacing Φ_B by Φ_e^c in Eqs. (2) and (3), respectively, \hbar is the reduced Planck constant. $\iota(y)$ and $\nu(y)$ are the correction factors due to image force barrier lowering [19], where y is the image force induced barrier lowering $\Delta\Phi_e^c$ normalized to Φ_e^c and is given by [14, 20]

$$y = \Delta\Phi_e^c / \Phi_e^c, \quad \Delta\Phi_e^c = \sqrt{\frac{q^3 E_{\text{ox}}}{4\pi\epsilon_{\text{ox}}^\infty}}. \quad (6)$$

$\epsilon_{\text{ox}}^\infty$ is the high-frequency permittivity of SiO_2 , ${}_2F_1$ is the Hypergeometric function [21] and $\eta = (\mathcal{E}_F - \mathcal{E}_{c,0}) / k_B T$. For a semiconductor, $(\mathcal{E}_F - \mathcal{E}_{c,0})$ changes as a function of the electric field across it, which in turn is related to the oxide electric field by the continuity condition of the electric displacement vector across the semiconductor/oxide boundary. Solving 1D Poisson's Equation in a semiconductor [14], η can be evaluated as a function of oxide field by solving

$$\frac{\epsilon_{\text{ox}}^2 E_{\text{ox}}^2}{2q\epsilon_{\text{sc}} k_B T} = N_c F_{3/2}(\eta), \quad (7)$$

where ϵ_{sc} and N_c are the permittivity and density of states in the CB of the semiconductor, respectively and F_j is the complete Fermi-Dirac integral of fractional order j and is given by [14]

$$F_j(\eta) = \frac{1}{\Gamma(j+1)} \int_0^\infty \frac{x^j dx}{1 + \exp(x - \eta)}, \quad (8)$$

where $\Gamma(j)$ is the Gamma function [21].

Our modified formula for FN tunneling from the accumulation layer governed by Eq. (5) is valid for $c < 1$ depending on T and E_{ox} as long as the cathode electric barrier remains triangular. In order to satisfy the condition $c < 1$, the lower limit of E_{ox} increases from 4.14 to 6.4 MV/cm when the temperature changes from 100 to 300 °C. As expected, the new analytical expression for J_{FN} is universal (independent of t_{ox} at a given temperature) for electron injection from the accumulation layer of a semiconductor having a given resistivity.

Using the CB offset values from independent band structure understanding as listed in Table 1 and employing Eq. (5), theoretically calculated J_{FN} from n^+ -polySi is observed consistently much smaller than the measured [8] J_G irrespective of temperatures and oxide thicknesses as illustrated in Fig. 3(a). Similar results are also presented in Fig. 3(b) during electron injection [3] at room temperature from non-degenerately doped n-type Si into SiO_2 films having varying thicknesses (20 to 105 nm). This was found to be true also with the CB offset values calculated using its value [14] of 3.25 eV for nominal doping at room temperature (not shown here). Oxide thickness independent J_{FN} shown in Fig. 3 exhibits a smaller thermal activation compared to that of the measured [3, 8] J_G . The observed effect was distinct and reproducible in several different occasions as reported during the write operation [20] of EEPROM devices under positive gate bias as well as during electron injection [13] from n-4H-SiC into thin SiO_2 and hence is not incidental.

The enhanced thermal activation of electron injection from the n^+ -polySi/ SiO_2 interface and oxide thickness depend-

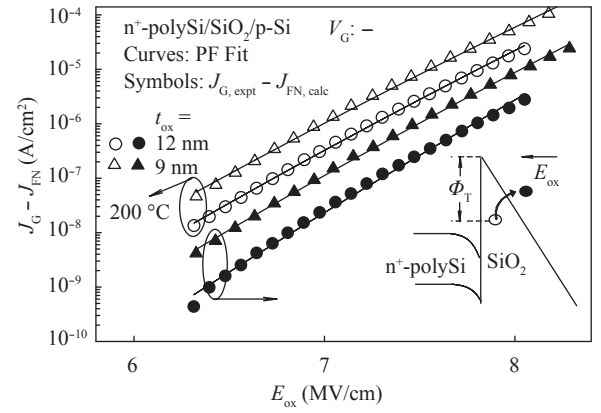


Fig. 4. Difference (symbols) between the absolute magnitudes of the measured J_G and the calculated J_{FN} at a given applied uniform oxide field with t_{ox} and temperature as parameters. Curves are fit to PF Eq. (9). Inset: schematic of the PF emission of electrons from oxide electron traps.

ency of the leakage current J_G indicate the presence of a thermally activated trap-assisted mechanism via Poole-Frenkel (PF) [22, 23] or Schottky emission (SE) [14] or two-step generalized trap-assisted tunneling (GTAT) [1] in these thin SiO_2 films. The GTAT model [1] is unlikely to be a candidate in explaining the strong temperature dependent J_G data because the trap concentration in as-grown devices does not change with ambient temperature as reported experimentally by Hadjadj *et al.* [8]. Moreover, the difference between the magnitudes of J_G and J_{FN} does not fit (not shown) with the equation [14] of SE. On the other hand, it is evident from Fig. 4 that $J_G - J_{\text{FN}}$ versus E_{ox} data fit well with the bulk-limited PF emission equation given by [13, 22]

$$J_{\text{PF}} = C_{\text{PF}} E_{\text{ox}} \exp\left(-\frac{q\Phi_T - \xi\beta_{\text{PF}} \sqrt{E_{\text{ox}}}}{k_B T}\right), \quad (9)$$

$$\beta_{\text{PF}} = \sqrt{q^3 / \pi\epsilon_0\epsilon_\infty},$$

where $J_{\text{PF}} (= J_G - J_{\text{FN}})$ is the PF current density, J_G is the measured leakage current density and J_{FN} is theoretically calculated FN current density using Eq. (5) at an identical applied field. C_{PF} is a constant depending on the density of electron traps and hence with t_{ox} as shown in Fig. 5(a), β_{PF} is the PF constant, ϵ_0 is the free space permittivity and $\epsilon_\infty = 2.15$ (square of refractive index) is the high-frequency dielectric constant of SiO_2 and Φ_T is the trap depth relative to the bottom of SiO_2 CB. The acceptor compensation factor ξ varies between 1 and 2 depending upon the amount of acceptor compensation [22] as depicted in Fig. 5(b). ξ was found to increase linearly with increasing oxide thickness and temperature. Indeed, during oxidation, near-interfacial neutral electron traps are created in the oxide. These traps emit electrons into the oxide CB under the application of an electric field at room temperature and above via the PF mechanism [23]. Φ_T can be determined from the Arrhenius plot of the intercepts of individual $\ln(J_{\text{PF}}/E_{\text{ox}})$ versus $\sqrt{E_{\text{ox}}}$ plots (also called PF plots) at a given T as illustrated in Fig. 5(a). The estimated

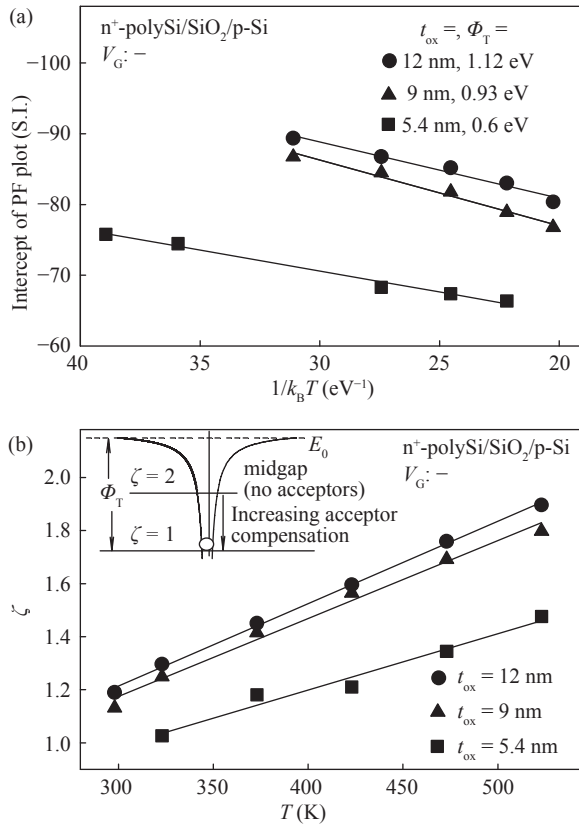


Fig. 5. (a) Arrhenius plot of the intercepts of the PF plots of the J_G - J_{FN} data for varying oxide thicknesses. (b) Temperature variation of the acceptor compensation factor ζ .

trap depth of 0.93 eV for 9 nm thick SiO₂ film agrees well with that reported by Harrell and co-worker^[23] for an identically thick MOS diode during negative gate injection. The estimated range of Φ_T between 0.6 to 1.12 eV is similar to the range of the metastable puckered configuration of oxygen vacancies in thermal SiO₂ as reported by Lu *et al.*^[24] from density functional theory. The results illustrated in Fig. 5(a) clearly shows that PF emission occurs from the deeper electron traps as well as the concentration of electron traps decreases resulting in C_{PF} being smaller with increasing oxide thickness. These cause a decrease in J_{PF} at a given E_{ox} and at a given T with increasing t_{ox} . We therefore speculate that very thick SiO₂ samples exhibit a universal (thickness independent) J_G - E_{ox} characteristic due to FN tunneling at a given temperature, where the contribution from PF electron emission is insignificant from energetically deep traps.

The classical PF Eq. (9) is physically meaningful till all the traps are ionized (emptied) and this happens at the saturation field E_{sat} obtained from the solution^[23] of $\partial^2 J_{PF} / \partial T^2 = 0$. Beyond E_{sat} , PF current is due to the drift motion of the carriers under the applied field and can be written as^[23] $J_{PF} = K n_r^{\max} E_{ox}$, where K is a constant, n_r is the free electron density in the conduction band relative to the effective density of states N_c and it attains maximum n_r^{\max} at E_{sat} . With increasing temperature, saturation in PF emission occurs at a lower field as can be seen in Fig. 6. Moreover, at a given temperature the saturation field E_{sat} exhibits a weak t_{ox} dependence (not shown). As evident from Fig. 6, E_{sat} is well above the intrinsic breakdown field of good quality SiO₂. A similar

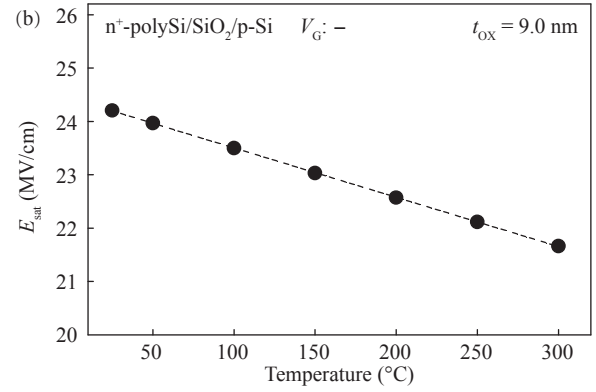


Fig. 6. Variation of the saturation field for PF emission with temperature during negative bias on n⁺-polySi gate. Curve is guide to eye only.

inference is drawn throughout the SiO₂ thickness range studied here between 25 and 300 °C. Therefore, measurement data cannot be extended up to the saturation field.

4. Conclusion

In conclusion, a comprehensive analysis is presented to understand the mechanisms of oxide thickness dependent electronic current conduction in thin SiO₂ films at a wide range of temperatures under negative bias on the n⁺-polySi gate. We propose that the measured leakage current from the n⁺-polySi gate is due to PF emission of electrons from the process-induced near-interfacial electron traps located in the oxide gap at energy levels between 0.6 and 1.12 eV below the SiO₂ CB for 5.4 to 12 nm-thick SiO₂ films in conjunction with FN tunneling of electrons from the accumulation layer of n⁺-polySi. We address that fitting the measured J_G versus E_{ox} data with the widely used LS Eq. (1) incorrectly explains the conduction mechanism solely due to FN tunneling at room temperature and above, where the thermally activated PF emission of trapped electrons from the near-interfacial neutral electron traps is a dominant factor responsible for the increase in leakage current.

A new modified expression has been proposed to calculate the FN tunneling current density as a function of temperature and applied electric field during electron injection from the accumulation layer of the semiconductor. A method is developed to segregate the above two current components I_{FN} and I_{PF} from the measured leakage current I_G , where I_{FN} from the accumulated semiconductor substrate can be estimated using our modified FN equation without any adjustable parameters and taking the small variation of CB offset Φ_c^c with temperature from the independent understanding of band structure physics instead of apparent thermal lowering of Φ_B obtained by fitting the measured J_G - E_{ox} data with LS Eq. (1) even exhibiting an excellent fit numerically. Our present work speculates the oxide thickness independent universal J_G - E_{ox} characteristics for very high quality thick oxides where the FN tunneling component significantly dominates the PF emission from energetically deep traps in the temperature range studied here. The present analysis can be extended to study the conduction mechanism under positive gate bias in MOS capacitors on n-type semiconductor substrate.

References

- [1] Yang B L, Lai P T, Wong H. Conduction mechanisms in MOS gate dielectric films. *Microelectron Reliab*, 2004, 44: 709
- [2] Lenzlinger M, Snow E H. Fowler–Nordheim tunneling into thermally grown SiO₂. *J Appl Phys*, 1969, 40: 278
- [3] Weinberg Z A. Tunneling of electrons from Si into thermally grown SiO₂. *Solid-State Electron*, 1977, 20: 11
- [4] Weinberg Z A. On tunneling in metal–oxide–silicon structures. *J Appl Phys*, 1982, 53: 5052
- [5] Krieger G, Swanson R M. Fowler–Nordheim electron tunneling in thin Si–SiO₂–Al structures. *J Appl Phys*, 1981, 52: 5710
- [6] Depas M, Vermeire B, Mertens P W, et al. Determination of tunneling parameters in ultra-thin oxide layer poly-Si/SiO₂/Si structures. *Solid-State Electron*, 1995, 38: 1465
- [7] Pananakakis G, Ghibaudo G, Kies R, et al. Temperature dependence of the Fowler–Nordheim current in metal–oxide–semiconductor structures. *J Appl Phys*, 1995, 78: 2635
- [8] Hadjadj A, Salace G, Petit C. Fowler–Nordheim conduction in polysilicon (n⁺)-oxide-silicon (p) structures: limit of the classical treatment in the barrier height determination. *J Appl Phys*, 2001, 89: 7994
- [9] Roca M, Laffont R, Micolau G, et al. A Modelisation of the temperature dependence of the Fowler–Nordheim current in EEPROM memories. *Microelectron Reliab*, 2009, 49: 1070
- [10] Aygun G, Roeder G, Erlbacher T, et al. Impact of temperature increments on tunneling barrier height and effective electron mass for plasma nitrided thin SiO₂ layer on a large wafer area. *J Appl Phys*, 2010, 108: 073304
- [11] Waters R, Zeghbroeck B V. On field emission from a semiconducting substrate. *Appl Phys Lett*, 1999, 75: 2410
- [12] Samanta P, Mandal K C. Leakage current conduction and reliability assessment of passivating thin silicon dioxide films on n-4H-SiC. *Proceedings of SPIE (SPIE, Bellingham, WA, 2016)*, 2016, 9968: 99680E
- [13] Samanta P, Mandal K C. Leakage current conduction, hole injection, and time-dependent dielectric breakdown of n-4H-SiC MOS capacitors during positive bias temperature stress. *J Appl Phys*, 2017, 121: 034501
- [14] Sze S M, Ng K K. *Physics of semiconductor devices*. New Jersey: John Wiley & Sons, Inc., 2007
- [15] Alay J L, Hirose M. The valence band alignment at ultrathin SiO₂/Si interfaces. *J Appl Phys*, 1997, 81: 1606
- [16] Afanasev V V, Bassler M, Pensl G, et al. Band offsets and electronic structure of SiC/SiO₂ interfaces. *J Appl Phys*, 1996, 79: 3108
- [17] Rossinelli M, Bosch M A. Reflectance spectrum of crystalline and vitreous SiO₂ at low temperature. *Phys Rev B*, 1982, 25: 6482
- [18] Persson C, Lindefelt U, Sernelius B E. Band gap narrowing in n-type and p-type 3C-, 2H-, 4H-, 6H-SiC, and Si. *J Appl Phys*, 1999, 86: 4419
- [19] Murphy E L, Good R H. Thermionic emission, field emission, and the transition region. *Phys Rev*, 1956, 102: 1464
- [20] Samanta P. Mechanistic analysis of temperature dependent current conduction through thin tunnel oxide in n⁺-polySi/SiO₂/n⁺-Si structures. *J Appl Phys*, 2017, 122: 094502
- [21] Wolfram Research, Inc., *Mathematica*, Version 11.0, 2016 (Champaign, IL)
- [22] Banerjee S, Shen B, Chen I, et al. Conduction mechanisms in sputtered Ta₂O₅ on Si with an interfacial SiO₂ layer. *J Appl Phys*, 1989, 65: 1140
- [23] Harrell W R, Gopalakrishnan C. Implications of advanced modeling on the observation of Poole–Frenkel effect saturation. *Thin Solid Films*, 2002, 405: 205
- [24] Lu Z Y, Nicklaw J, Fleetwood D M, et al. Structure, properties, and dynamics of oxygen vacancies in amorphous SiO₂. *Phys Rev Lett*, 2002, 89: 285505